



Audio Engineering Society

Convention Paper 10617

Presented at the 153rd Convention
2022 October

This paper was peer-reviewed as a complete manuscript for presentation at this convention. This paper is available in the AES E-Library (<http://www.aes.org/e-lib>) all rights reserved. Reproduction of this paper, or any portion thereof, is not permitted without direct permission from the Journal of the Audio Engineering Society.

Simulating low frequency noise pollution using the parabolic equations in sound reinforcement loudspeaker systems

Thomas Mouterde¹, Joris Perrot¹, Bertrand Lihoreau², and Etienne Corteel¹

¹*L-Acoustics, 13 rue Levacher Cintrat, 91460 Marcoussis, France*

²*Laboratoire d'Acoustique de l'Université du Mans (LAUM, UMR CNRS 6613), 72085 Le Mans, France.*

Correspondence should be addressed to Thomas Mouterde (thomas.mouterde@l-acoustics.com)

ABSTRACT

Sound system designers are used to optimizing loudspeaker systems for the audience experience with free-field simulation software. However, noise pollution reduction must also be considered during the design phase and the propagation of sound may be affected by inhomogeneous atmospheric conditions, such as wind, temperature gradients, and ground impedance. This paper proposes a method to simulate the impact of the environment on sound pressure levels at large distances created by loudspeaker systems using parabolic equations, considering a reference left-right main system associated with either flown or ground-stacked subwoofers. Results show a higher variability of the sound pressure level with systems using ground-stacked subwoofers. The influence of the crossover frequency between main and subwoofers is discussed in this paper.

1 Introduction

When designing a sound reinforcement loudspeaker system, the first requirement is to provide the audience with the best sound experience. It consists mainly of a consistent and homogeneous Sound Pressure Level (SPL) distribution and frequency response throughout the audience area. In addition, the sound system designer must account for the audience and workers' auditory health and address noise pollution issues. This last element, dealing with the SPL generated by the loudspeaker system at large distances, is increasingly considered, especially for outdoor events [1].

This paper builds on a previous study [2] that considered the polar pattern of large-scale sound reinforcement systems in free field, comparing various subwoofer arrangements in combination with a reference left-right system. The study further investigates the

influence of atmospheric conditions on propagation effects considering only omnidirectional sound sources at 40 Hz. The results indicate that downwind conditions (wind going in the propagation direction) or positive temperature gradients increase the SPL at large distances. On the contrary, upwind conditions (wind opposing the propagation direction) or negative temperature gradients decrease the SPL at large distances. Moreover, the results indicate a higher impact of the speed of sound gradient on SPL at large distances for ground-stacked rather than flown sources.

However, sound system designers typically use free-field simulations only, not accounting for atmospheric conditions variations (wind or temperature gradient) or the environment (ground nature). This paper has therefore two objectives. It first proposes a computationally efficient method to test the influence of inhomogeneous atmospheric conditions and ground nature on far-field

sound propagation of realistic loudspeaker systems at low frequencies. Frequencies between 20 and 160 Hz are considered, with a sufficient frequency resolution ($1/6^{\text{th}}$ octave). The second objective of the paper is to compare typical loudspeaker system designs regarding noise pollution. The first part of this paper presents the loudspeaker system configurations under study and the evaluation metrics. The second part introduces a novel method based on 3D Parabolic Equations (3DPE). Parabolic equation (PE) [3] is a very accurate method for propagation computation in complex domains. In the last part, simulation results are presented and discussed.

2 Loudspeaker system design

2.1 Systems setup

The loudspeaker systems considered here are consisting of a full-range main left/right system combined with either flown or ground-stacked subwoofers. The main system is composed of 12 L-Acoustics K2 per side, flown at 9 m, spaced 18 m apart. Both subwoofer configurations are composed of 16 L-Acoustics KS28: 8 subs per side, flown as two vertical lines with 22 m spacing for the *Sub Beside* configuration; 8 columns of 2 subs, spaced of 2 m for the *Arc Sub*, see Figure 1. These are the two configurations that provide the best side rejection according to [2].

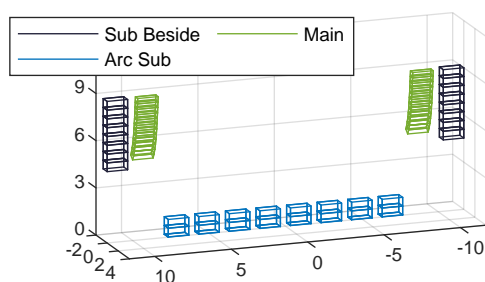


Fig. 1: Overview of the main system and the two tested subwoofer configurations.

The crossover between the main and the subwoofers of both configurations is originally around 60 Hz (systems named *Sub Beside 60* and *Arc Sub 60*). Both combinations are also investigated with crossovers shifted toward 100 Hz (named *Sub Beside 100* and *Arc Sub 100*). A preset with a 100 Hz cutoff frequency is selected for subwoofers and a high pass filter at 100 Hz

is applied to the main system (Linkwitz–Riley order 4), see Figure 2.

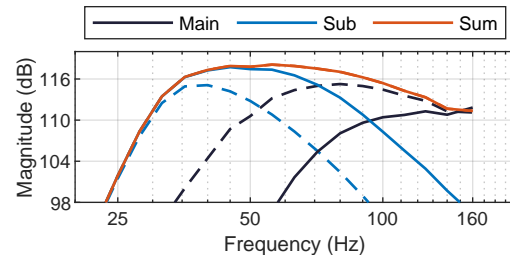


Fig. 2: Crossover between main and subs (*Sub Beside*): original crossover (dashed line), and modified crossover around 100 Hz (continuous line).

Loudspeaker systems are modeled by several point sources. Each point source is described by a complex directivity computed from measurements of L-Acoustics loudspeakers. This Complex Directivity Point Source (CDPS) model, see [4], is commonly used in free-field simulation software. Simulations are performed at monochromatic frequencies each sixth of octave, between 22.4 and 160 Hz. The 31.5, 63, and 125 Hz octave bands (averaged out of 6 frequencies) are inspected in the following. Additionally, the A-weighted average level over the 25 – 160 Hz frequency range is computed. This A-weighted SPL is most of the time used in regulations [1].

2.2 Comparison method

As mentioned in [2], systems can only be compared if they provide the audience with the same mean frequency response. A drive signal is computed for each system so that all systems reach the same target spectrum at 40 m, at the front of the system (averaged in $\pm 30^\circ$ around the axis). The target spectrum, described in [5], corresponds to the spectrum measured at the front-of-house mixing position of several large stages for outdoor events (47 concerts), see Figure 3. The level is set to 99 dBA or 112 dBC. These levels are realistic and quite common at a concert.

In the following, systems are compared using their polar responses computed at 250 m from the origin. The ground is assumed to be flat and the pressure is measured at 2 m height. For a deeper analysis of the directivity of the systems, the space is divided into angular portions as proposed in [2]: the *front*, $\pm 30^\circ$

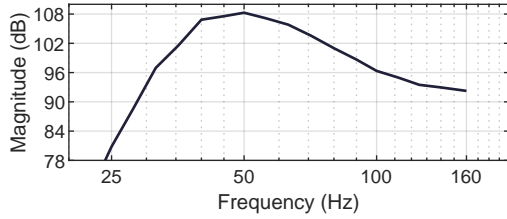


Fig. 3: Mean spectrum measured at FOH (47 concerts) from [5], with an SPL of 99 dB(A) or 112 dB(C), used as target for all systems.

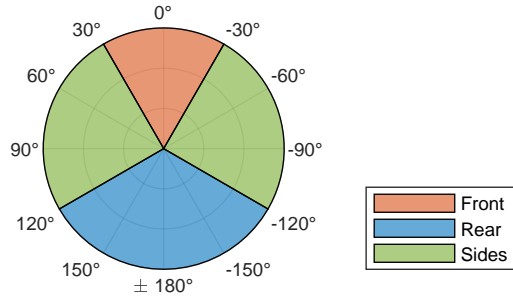


Fig. 4: Illustration of the division of the space in several angular portions.

around the system axis, the *rear*, $\pm 60^\circ$ behind the system, and the *sides*, see Figure 4. The *front* typically corresponds to the far-field level created in the direction of the audience area. The *front* is evaluated considering the absolute averaged SPL (frequency and space). Even though levels are normalized around a reference position in reference conditions, the *front* SPL can be affected by atmospheric conditions depending on chosen subwoofer placement and crossover frequency. The *sides* typically corresponds to off-site locations that can be affected by noise pollution, primarily at low frequencies. As shown in [2], the design choices of the subwoofer system under investigation can affect the *sides* SPL. For *sides*, the relevant comparison metric is the side rejection: difference between the *front* average SPL and the *sides* average SPL under the same atmospheric conditions. The *rear* portion is only very little affected by the subwoofer positioning and crossover settings for the loudspeaker systems considered here [2]. Therefore, it is not considered in the simulations.

3 Simulation method

3.1 Parabolic equation method

The parabolic equation (PE) in two dimensions is obtained from the Helmholtz equation in harmonic regime:

$$\left[\frac{\partial^2}{\partial x^2} + \frac{\partial^2}{\partial z^2} + k_0^2 \right] p(x, z) = 0, \quad (1)$$

where x is the direction of propagation, z is the height of the domain, $k_0 = \omega/c_0$ is the wave number with c_0 the speed of sound. A $e^{-j\omega t}$ time dependence is assumed throughout this paper. By choosing a principal direction of propagation (mostly in the x direction) without backpropagative wave, and considering a stratified domain according to z , it is deduced two parabolic equations characterizing the propagation of the wave toward increasing x and toward decreasing x direction ([6] and [7]):

$$\left(\frac{\partial}{\partial x} \pm jk_0 Q \right) p^\pm(x, z) = 0, \quad (2)$$

where $Q = \sqrt{1 + \frac{1}{k_0^2} \frac{\partial^2}{\partial z^2}}$ is the propagation operator. The one concerning the propagation toward the positive x direction uses the negative sign, and conversely.

The development of the propagation operator Q brings a certain angular validity. To obtain an equation with a great angle of validity compared to the propagation axis (about 30 - 40°), a Split-Step Padé (1,1) method is used to develop the Q operator [7]. The resulting equation is called Wide Angle Parabolic Equation (WAPE). It can then be integrated numerically between x and $x + \Delta x$ thanks to a Crank-Nicholson scheme and a centered finite difference scheme of the second order for z variable (height).

A three-dimensional parabolic equation (3DPE) method has been developed for street canyon propagation [6] and is adapted in the following. To solve the PE in 3D, the Alternating Direction Implicit (ADI) method is used in order to transform a partial differential equation of several dimensions into a composition of first-order differential equations. It consists in reformulating the 3DPE in two series of 2D WAPE representing the evolution of the pressure field according to y axis (width) and z axis (height). The same numerical schemes mentioned previously are used to solve

them according to propagation direction (x axis). The acoustic field is computed from $x = x_0$ to $x = x_0 + \Delta x$ as follows. The field is discretized into $M_z \times M_y$ matrix (a step $\Delta x, y, z = \lambda/10$ is chosen as advised in [3]). Firstly, M_y columns of the matrix are propagated from $x = x_0$ to a fictitious point located at $x = x_0 + (\Delta x/2)$. Then, M_z rows are propagated from $x = x_0 + (\Delta x/2)$ to $x = x_0 + \Delta x$ (see Figure 5). The resolution of these equations is based on typical matrices inversions as LU decomposition and offers quite good calculation time for large domains.

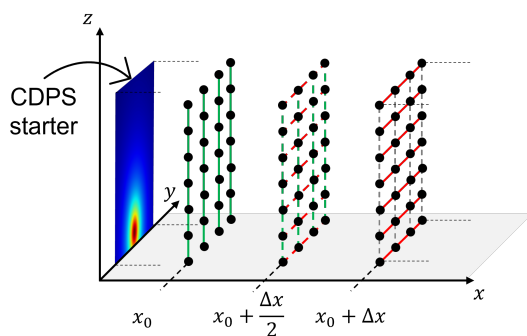


Fig. 5: Illustration of the 3DPE recursion scheme.

To simulate a free field on the sides and the top of the domain (sky), a damping function of Gaussian type (detailed in [7]) is used to avoid parasitic reflections on domain boundaries. This function is applied on all boundaries of the domain except the ground with a size ratio of 40%.

3.2 Starting field

The parabolic equations propagate a pressure field and need an initial source condition called starter. With 3DPE, a 2-dimensional pressure field is required. Usually, Gaussian sources are used to simulate monopoles for several reasons explained in G.12 of [3]. In that study, the aim is to simulate different designs of real sources. The possibility to use a starter from a loudspeaker system is investigated in the following part.

The pressure field generated by a loudspeaker system is computed analytically in the vertical plane at 30 m from sources with the CDPS model. To take into account the effect of the environment from the origin of the systems, the pressure field is firstly propagated from 30 m (CDPS starter) to the origin, using the backward propagation method described in [8]. Homogeneous

neutral atmospheric conditions are assumed during the back-propagation. This pressure field can then be used as the starter for the propagation using the classical PE method, with any atmospheric condition.

To obtain the best simulation accuracy and sufficient validity along width and length (because of damping functions), different sizes of starters were tested. The chosen sizes are 200 m in width per 100 m in height. However, for frequencies below 50 Hz, to keep a good simulation accuracy, the size needs to be increased to dimensions depending on the frequency. The size of the starter is then 300 steps (Δy) by 150 steps (Δz).

3.3 From pressure field to polar

The objective of the present study is to compare systems using polar responses computed at 250 m, but the 3DPE method allows for computing a pressure field in a given direction, with a limited angle of validity. Several starters are computed analytically all around the systems to overcome this limitation. Pressure fields are then calculated in each direction using 3DPE. The polar response is finally reconstructed picking up pressure values in each of these fields, see Figure 6.

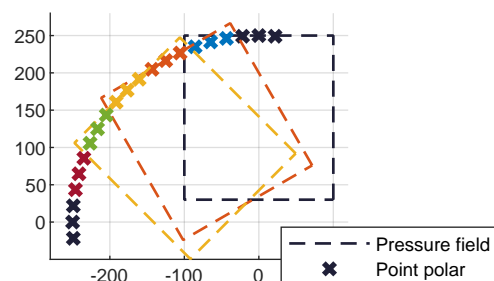


Fig. 6: Illustration of the method used to compute polar responses from pressure fields computed with the 3DPE method.

A compromise needs to be found between pressure fields width, angle of validity of 3DPE, and angle step between directions. Good efficiency is obtained with pressure fields width of 200 m. It remains a useful area of ± 20 m around the axis because of the Gaussian damping function. At 250 m, it corresponds to $\pm 5^\circ$. This angle is below the 3DPE validity angle. Pressure fields are thus computed each 15° around the systems, up to 250 m. As illustrated in Figure 6, 3 values of the polar response are extracted from each pressure field:

the values on-axis and at $\pm 5^\circ$ around the axis. For instance, with the pressure field computed in the 30° direction of the system, values of the polar response at 25° , 30° , and 35° are extracted, in orange in Figure 6. Linear interpolation is used when the desired point does not correspond to the mesh. The polar response of the *sub beside* configuration computed with the proposed method is presented in Figure 7 for three frequencies.

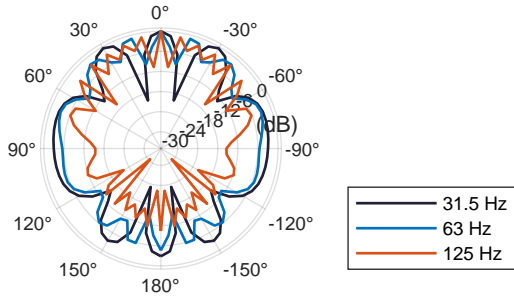


Fig. 7: Polar response at 3 monochromatic frequencies, 3DPE method, *Sub Beside* configuration.

3.4 Assessment of the method

The validity of the proposed method is investigated by comparing the polar responses thus obtained with the polar responses computed analytically. The analytical polar responses are computed in Matlab, using the same method as the one used to compute the starters for 3DPE (CDPS model with loudspeaker data). An image source is used to simulate the reflection on the ground for the analytical model and a fully reflective ground is simulated in the PE method.

Comparisons between polar responses computed analytically and using 3DPE for all system combinations (main system associated with each subwoofer configuration) are investigated in Figure 8. It presents an overview of the SPL difference between the analytical and 3DPE models at each frequency in each direction ($\pm 20^\circ$ around the displayed direction are considered). Considering all frequencies (18) and all directions (72), the SPL difference between both methods is quite small, in most cases well below 1 dB. Some artifacts remain at some frequencies for some angles. It can be explained, for instance, by small differences at interference positions. Indeed, the numerical method implies a meshing of the space. It can lead to mistakes in the case of very localized cancellations. However, the overall method

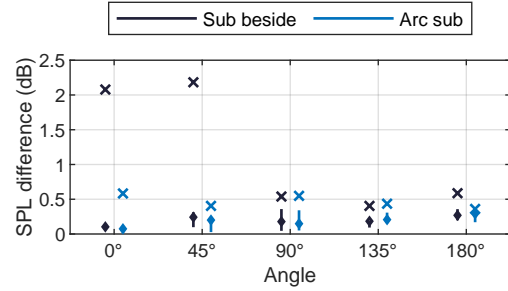


Fig. 8: SPL difference between analytical solution and 3DPE: median (diamond), 25th - 75th percentile interval (vertical bars), 95th percentile (x).

used to compute polar responses from starters in several directions, and propagated using 3DPE proves its efficiency. This method is used in the following to simulate the impact of the environment.

3.5 Environment simulation

Atmospheric conditions are generally inhomogeneous. As described in [2], the wind speed and the temperature vary with the altitude, creating a speed of sound gradient. The vertical celerity profile is accounted for by introducing the variable ε in 3DPE, which represents the variations of the refraction index of the medium. ε is defined by:

$$\varepsilon = (c_0/c_{eff})^2 - 1, \quad (3)$$

with c_{eff} , the effective speed of sound, and c_0 is the reference speed of sound. The variable Q in equation (2) becomes:

$$Q = \sqrt{1 + \varepsilon + \frac{1}{k_0^2} \frac{\partial^2}{\partial z^2}}. \quad (4)$$

In the following, the celerity profiles are determined with a hybrid method developed for the European research project Harmonoise [9]. This method allows computing in each propagation direction the effective speed of sound vertical profile:

$$c_{eff}(z) = c_0 + a_{log} \cdot \ln\left(1 + \frac{z}{z_0}\right) + b_{lin} \cdot z, \quad (5)$$

with z the altitude, c_0 the speed of sound at ground level, and z_0 the ground roughness length (typical values available in [9]). The parameters a_{log} and b_{lin} are

computed from observations and a few measurements close to the ground: temperature, wind speed, wind direction, period of the day, and cloud cover. Figure 9 presents the speed of sound profiles used in this study. All simulations are performed without cloud covering and at a temperature at ground level of 20°C. The first simulations compare the speed of sound profiles of a day versus a night, without wind. On a sunny day, the sun warms the ground and the heat is transferred to the air close to the ground. On the contrary, during the night, the heat is absorbed by the ground, and the air close to the ground is cooled. A temperature gradient is thus created and modified between the day and the night. This phenomenon so-called "temperature inversion" is quite common at outdoor summer festivals.

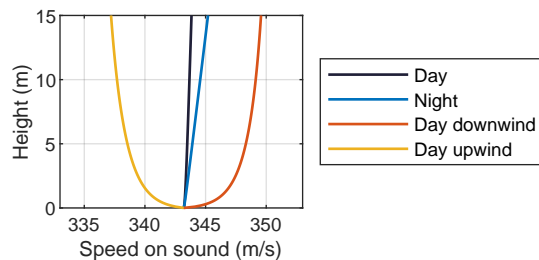


Fig. 9: Speed of sound profiles in various atmospheric conditions used in the following simulations.

Simulations with wind are performed in day conditions. The wind is defined at 8 m/s at 10 m height. The ground roughness length is set at 0.15 m, see [9], it corresponds to a typical terrain for an open-air festival. As can be observed in Figure 9, the speed of sound variations due to wind and temperature changes are limited (<2%). The effective speed of sound approximation is valid in a stratified atmosphere if the wind speed is small compared to the speed of sound and if the elevation angle is small (source and receiver close to the ground), see [3]. Such conditions are fulfilled in the context of this study, allowing to consider the medium as motionless and to express the speed of sound gradient as only depending on altitude.

A short-term scale is considered for the meteorological data aspect which involves neglecting turbulence as explained in [9]. Turbulence could be considered in 3DPE but it would imply a very long calculation time. The potential effect of turbulence would be to mitigate strong cancellations, especially in the shadow zone

created by a strong negative speed of sound gradient, see [9]. A strong reduction of the SPL will be observed neglecting turbulence, which would not be observed in reality. As a consequence, results in the upwind situation must be considered very carefully.

The impedance of the ground is introduced in the 3DPE as a normalized admittance $\beta = Z_c/Z_g$, where $Z_c = \rho_0 c_0$ is the characteristic impedance of the air and Z_g is the impedance of the ground. Z_g is determined thanks to Delany-Bazley-Miki model [10]. This model allows estimating the ground impedance in realistic conditions depending on the frequency and static air flow resistivity of the ground σ in Nm^{-4}s . A perfectly reflective ground is used for simulations studying the impact of the temperature and wind gradients. The impact of the ground impedance is studied afterward.

4 Simulation results

4.1 Impact of the temperature

The impact of the temperature is similar in all directions. The *front* SPL is shown in Figure 10 comparing day and night conditions without wind.

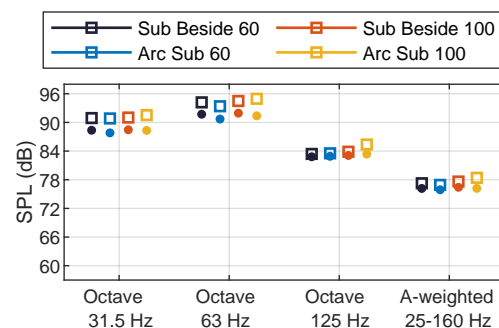


Fig. 10: *Front* SPL without wind: day (points) and night (square) temperature conditions.

During the day, the level is similar for all system configurations in the 31.5 and 125 Hz octave bands, while in the 63 Hz octave band, the level is slightly smaller with an arc sub (-1 dB than the *Sub Beside 60*). The SPL in dBA over the band 25 – 160 Hz is similar for all system configurations. The SPL increases during the night for all configurations and in all octave bands. This level increase is higher for configurations using an arc sub, especially with the crossover at 100 Hz. Consequently, this configuration presents the highest SPL

during the night in all studied octave bands (resulting in an SPL(A) 1.2 dB higher in the band 25 – 160 Hz).

4.2 Wind on the system axis

Figure 11 presents the *front* SPL under two wind conditions: when the wind blows toward the front of the system (downwind, "+") and when the wind blows toward the rear of the system (upwind, "-"). These two conditions represent the two extreme cases and any other wind direction would lead to a *front* SPL between the "+" and the "-" symbols of Figure 11.

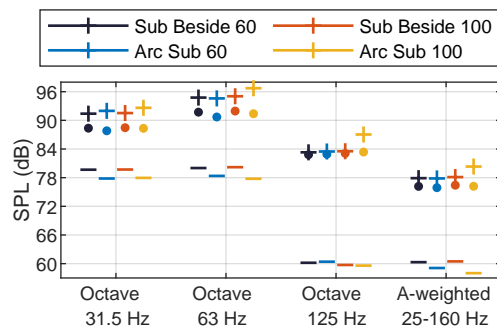


Fig. 11: *Front* SPL with on-axis wind: downwind ("+"), upwind ("-"), no wind (points).

Several observations can be made:

- the level increases under downwind conditions and decreases under upwind conditions, compared to no wind conditions, it is observed for all configurations and in all studied octave bands;
- the level at the front is slightly smaller with arc sub configurations without wind, but becomes similar, or even higher, in downwind conditions, especially if the crossover is set at 100 Hz (respectively +2 dB and +4 dB in the 63 Hz and 125 Hz octave bands compared to the *Sub Beside 60*);
- downwind, over the band 25 – 160 Hz, the SPL(A) is 2.5 dB higher with the *Arc Sub 100* than with other configurations.

For further investigation, the impact of the wind on single systems is presented in Figure 12. It shows the level difference between downwind and no wind conditions for the systems alone: the subwoofers and the main system are inspected separately.

It can be observed that the wind increases the SPL for all sources at very low frequencies. However, the

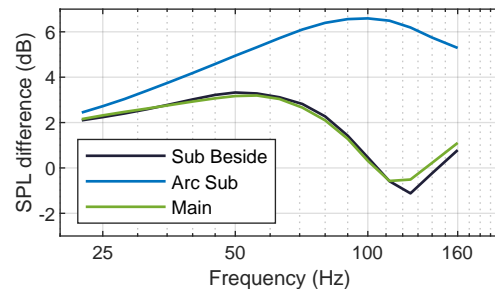


Fig. 12: *Front* SPL difference between downwind and no wind conditions, main and subwoofer systems separately.

influence of the wind starts to decrease at 50 Hz for a flown source while the wind continues to increase the SPL for a ground-stacked source up to 100 Hz. It explains the higher variability of SPL for combinations using an arc sub, especially with a crossover at 100 Hz, a larger frequency range being reproduced by a ground-stacked source. The smaller SPL variability with flown sources can be explained by the smaller speed of sound gradient observed at higher altitudes, see Figure 9.

To summarize, the variability due to the downwind condition can be compared by octave bands. In the 31.5 Hz octave band, 4 dB are added to the SPL at the front for both arc sub configurations, versus 3 dB for flown configurations. In the 63 Hz, 4 dB and 5.5 dB are respectively added for the *Arc Sub 60* and *Arc Sub 100*, versus 3 dB for flown configurations. In the 125 Hz octave band, 4 dB are added for the *Arc Sub 100* configuration while less than 1 dB is added for other configurations.

4.3 Wind perpendicular to the system axis

A lateral wind blowing perpendicularly to the system axis is now considered (toward the 90° direction on a polar plot). Figure 13 shows the polar response of the main system associated with both subwoofer configurations (60 Hz crossover), averaged over the 25 – 160 Hz frequency range, without wind (dashed line) and with a lateral wind (continuous line). As expected, the level increases downwind (left side) and decreases upwind (right side). The interference pattern directions are stable. The level on the left side is slightly smaller with the *arc sub* without wind, but almost similar with the wind. The arc sub configuration is more affected by the wind, especially on the upwind side.

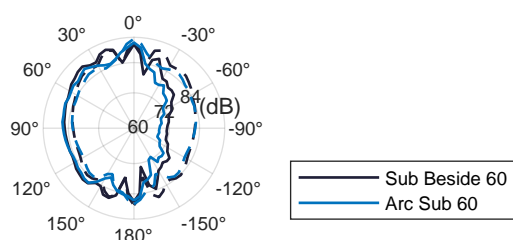


Fig. 13: Polar response (25 – 160 Hz), *Sub Beside 60* and *Arc Sub 60* configurations: without wind (dashed lines), with lateral wind at 90° (continuous line).

Figure 14 presents the rejection at the sides of the systems. The point represents the value without wind, while the "+" and the "-" represent the values on the sides downwind and upwind respectively.

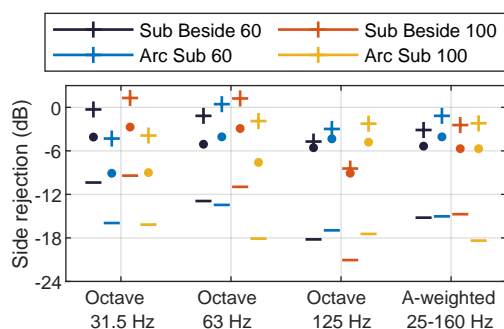


Fig. 14: Side rejection with lateral wind (90°): downwind ("+"), upwind ("-"), no wind (points).

In the 31.5 Hz octave band, the arc sub configurations present the best side rejection. This is true for any wind condition. In the 63 Hz octave band, the rejection of the *Arc Sub 60* is not better than the *Sub Beside 60*, even worse especially under downwind conditions. The *Arc Sub 100* presents the best side rejection without wind. The shifted crossover extends the capability of the arc sub to control the directivity. However, the side rejection of the *Arc Sub 100* is widely impacted by the wind. The rejection at the downwind side is reduced by 6 dB and becomes almost similar to the rejection of the *Sub Beside 60*. In the 125 Hz octave band, the *Sub Beside 100* has the best side rejection. This rejection is created by the interaction between the main and

subwoofer systems. The shifted crossover improves the rejection in this octave band (but also reduces it in the 63 Hz octave band). This rejection is, moreover, stable downwind. Both arc sub configurations present a worse side rejection than the *Sub Beside* configurations in 125 Hz octave band. Finally, the *Arc Sub 60* presents the worst side rejection in the A-weighted 25 – 160 Hz band, whatever the wind conditions. The *Arc Sub 100* presents a similar side rejection than both *Sub Beside* configurations without wind, but a slightly worse rejection downwind.

4.4 Influence of the ground impedance

The next simulation parameter under test is the influence of the ground impedance and its interaction with the wind. Downwind conditions are particularly investigated because the downward refraction thus created concentrates the sound close to the ground. The ground impedance is computed based on the flow resistivity of the ground. Two typical values are studied here: 200 kNm⁻⁴s representing an uncompacted ground as pasture field (soft ground) and 20000 kNm⁻⁴s corresponding to a hard surface as asphalt or concrete (hard ground), see [11]. The SPL difference at the front of the system between downwind and no wind conditions for both ground impedances is displayed in Figure 15.

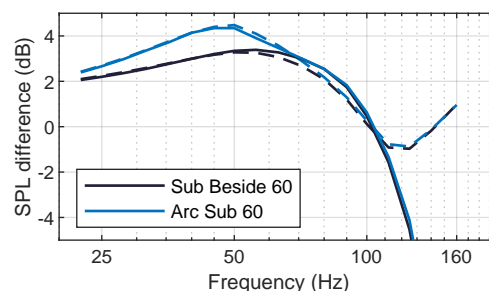


Fig. 15: Front SPL difference between downwind and no wind conditions: soft ground (continuous lines) and hard ground (dashed lines).

Results show that the influence of wind changes with the impedance of the ground according to frequency. Below the crossover frequency, the arc sub configuration is more impacted by the wind than the flown configuration, whatever the ground properties. It confirms the previous observations done in section 4.2. Above the crossover frequency, the SPL difference is the same for both subwoofer configurations due to the

bigger contribution of the main system. Furthermore, the ground class influences the slope of the decrease above the crossover frequency, the influence of the wind being higher with a soft ground with an SPL reduction compared to the no wind condition. In the crossover region, some differences between subwoofer design choices can be observed but remain limited, less than 0.5 dB for a given ground class.

5 Discussion

Simulations are performed using 3D Parabolic Equations. 3DPE is a very accurate method for wave propagation in realistic conditions [3] with a highly reduced computational cost compared to other advanced computational methods such as FEM. This method has been generally used in underwater acoustics and was then presented for atmospheric acoustics in 1989 by Gilbert & White [12]. 3DPE can simulate complex sources, accounting for variable ground impedance and vertical celerity profiles, with increased accuracy compared to ray acoustics methods, especially at low frequencies.

The benefits of simulations compared to field measurements is the availability to control atmospheric conditions and describe precisely the influence of individual parameters such as:

- wind direction,
- wind speed,
- temperature changes,
- ground physical properties.

The use of the effective speed of sound approximation describes these variations as a speed of sound gradient that varies only with altitude and not with the direction of propagation in other dimensions. This approximation means that the location of interference patterns is not affected by varying atmospheric conditions. The observed far-field polar pattern is therefore affected either globally (temperature or ground nature changes), compressed or expanded in a smooth direction dependent manner (wind from a specific direction). This approximation is justified in section 3.5.

The 3DPE simulations of a realistic left/right large scale loudspeaker system show a higher impact of wind or temperature gradients on far-field SPL for ground stacked sources compared to flown sources (see Figures 10, 11, 12, and 14). This confirms the observations made in [2] using Finite Element Method and ray acoustics simulations with ideal point sources. Moreover, a

similar larger variability of SPL at low frequencies has been observed in the audience area for ground-stacked compared to flown sources depending on the audience density [13].

The proposed method offers also a more accurate description in the frequency domain, because of the limited processing power requirements, with a $1/6^{th}$ octave band resolution. It is therefore shown that the influence of temperature and wind is higher for ground-stacked sources compared to flown sources, especially in the 50 – 100 Hz frequency range. A larger amount of energy coming from a source on the ground results in a larger modification of the SPL at large distances with inhomogeneous atmospheric conditions. The most important variations are thus observed when ground-stacked subwoofers are used with a high crossover frequency (at 100 Hz in the present study).

Wide level reductions are observed in upwind conditions (Figures 11 and 14). A shadow zone is created. This could be useful for noise pollution reduction if prevailing winds put residential neighborhoods in upwind conditions. However, turbulence is not simulated in this study and the level reduction would be smaller in reality. A smaller level reduction can be observed, for instance in [2], with simulation using the Nord2000 standard. Indeed, in the Nord2000 standard, see [11], a reflection effect contribution is added in the shadow zone to improve the estimation of the SPL.

The ground properties influence the impact of the wind on the SPL at large distances. However, the interaction between these two parameters is limited to a small frequency range and restricted to small SPL differences in downwind conditions (<1 dB). Consequently, a perfectly reflective ground is a good approximation to simulate the impact of the speed of sound gradient at low frequencies.

6 Conclusion

This study builds on a previous paper that compared subwoofer configurations regarding noise pollution in free-field conditions or with a point source model to illustrate the influence of inhomogeneous atmospheric conditions on sound propagation [2].

A simulation method is presented here to investigate the impact of the environment at low frequencies on large-scale sound reinforcement systems combining flown

full-range line sources with either flown or ground-stacked subwoofers, with varying crossover frequencies. Three-Dimensional Parabolic Equations (3DPE) are used for their ability to consider various atmospheric conditions and ground properties. A flat listening area is considered, without any obstacles, and with a stratified atmosphere. The proposed method uses real loudspeaker systems models as sources (starter), improving the simulation accuracy compared to [2]. Starters are computed in several directions and propagated using 3DPE up to 250 m from systems. Polar responses are finally reconstructed from the pressure fields.

Higher variability in far-field SPL with varying atmospheric conditions is observed with configurations using ground-stacked sources compared to flown sources, especially with a high crossover frequency (100 Hz here). An arc sub can be efficient to reduce the noise pollution at the sides of the system at very low frequencies (31.5 Hz octave band), which are however largely ignored by noise pollution regulation [1]. Overall, the bandwidth of ground-stacked sources must be limited to reduce the SPL variations due to changing atmospheric conditions.

It has been highlighted in [2] that noise pollution issues should be considered with audience experience and auditory health. The conclusion regarding noise pollution is in agreement with the conclusions regarding those two other topics. Overall, flown subwoofers appear to be the best compromise.

References

- [1] Hill, A. J., “Understanding And Managing Sound Exposure And Noise Pollution At Outdoor Events,” in *AESTD1007.1.20-05.*, 2020.
- [2] Mouterde, T. and Corteel, E., “On the comparison of flown and ground-stacked subwoofer configurations regarding noise pollution,” in *Audio Engineering Society Convention 151*, Audio Engineering Society, 2021.
- [3] Salomons, E. M., *Computational atmospheric acoustics*, Springer Science & Business Media, 2001.
- [4] Feistel, S., *Modeling the Radiation of Modern Sound Reinforcement Systems in High Resolution*, Logos Verlag Berlin GmbH, 2014, ISBN 978-3-8325-3710-4.
- [5] Ederer, H.-J., Händel, M., Nicht, A., Roy, A., Seifert, S., Stüber, C., Trepte, H., and Zschaler, H., “Ergänzung zur Sächsischen Freizeitlärmstudie,” 2019.
- [6] Doc, J.-B., Lihoreau, B., Félix, S., Faure, C., and Dubois, G., “Three-dimensional parabolic equation model for low frequency sound propagation in irregular urban canyons,” *The Journal of the Acoustical Society of America*, 137(1), p. 310–320, 2015.
- [7] Blairon, N., *Effets de la topographie sur la propagation des ondes acoustiques dans l’atmosphère: modélisation avec l’équation parabolique et validation sur un site extérieur*, Ph.D. thesis, Écully, École centrale de Lyon, 2002.
- [8] Collins, M. D. and Westwood, E. K., “A higher-order energy-conserving parabolic equation for range-dependent ocean depth, sound speed, and density,” *The Journal of the Acoustical Society of America*, 89(3), pp. 1068–1075, 1991.
- [9] Gauvreau, B., Ecotière, D., Lefèvre, H., and Bonhomme, B., *Propagation acoustique en milieu extérieur complexe, caractérisation expérimentale in-situ des conditions micrométéorologiques, éléments méthodologiques et météorologiques*, Laboratoire central des ponts et chaussées, 2009.
- [10] Miki, Y., “Acoustical properties of porous materials-Modifications of Delany-Bazley models,” *Journal of the Acoustical Society of Japan (E)*, 11(1), pp. 19–24, 1990.
- [11] Plovsing, B., “Proposal for Nordtest Method: Nord2000 - Prediction of outdoor sound propagation,” Technical report, Nordic Noise Group, 2014.
- [12] Gilbert, K. E. and White, M. J., “Application of the parabolic equation to sound propagation in a refracting atmosphere,” *The Journal of the Acoustical Society of America*, 85(2), p. 630–637, 1989.
- [13] Mouterde, T., Corteel, E., and Melon, M., “Audience effect on the response of a loudspeaker system in the low frequency range, part 1: magnitude,” in *Audio Engineering Society Convention 149*, 2020.